our samples were just between two and three dimensions. We also found two filaments that were joined[4].

For magnetic fields between 0.7 and 4.5 mT, a single filament dragged adjacent ones along, forming rivers[7] (Fig. 2c, d) that intermittently changed their location and width.

To investigate stronger interactions between vortices, we increased the temperature instead of the magnetic field, as we could not observe vortices individually above 4.5 mT owing to the overlap of their magnetic fields, and found a new form of plastic flow, which we designate distorted-lattice flow. At 50 K, and with a magnetic field exceeding 1.5 mT, the vortex lattice was divided into domains that tended to move separately because of non-uniform pinning. Sometimes one domain was suddenly displaced slightly with respect to its neighbouring domains, producing edge dislocations (Fig. 2e, f); sometimes all of the vortices in one domain disappeared while the vortices rearranged during the slip, before reappearing as different lattice orientations were formed (Fig. 2g, h). Under these conditions, vortices generally proceeded in units of domains, sometimes with slips between domains or with changing lattice orientations.

A. Tonomura*‡, H. Kasai*, O. Kamimura*, T. Matsuda*, K. Harada*‡, J. Shimoyama†‡, K. Kishio†‡, K. Kitazawa†‡

**Advanced Research Laboratory, Hitachi Ltd, Hatoyama, Saitama 350-0395, Japan*
e-mail: tonomura@harl.hitachi.co.jp
†Department of Applied Chemistry, University of Tokyo, Tokyo 113-8656, Japan
‡CREST, Japan Science and Technology Corporation (JST), Kawaguchi, Saitama 332-0012, Japan

1. Harada, K. *et al. Nature* **360,** 51–53 (1992).
2. Kotaka, Y. *et. al. Physica C* **235–240,** 1529–1530 (1994).
3. Crabtree, G. W. & Nelson, D. R. *Phys. Today* **50**(4), 38–45 (1997).
4. Grønbech-Jensen, N., Bishop, A. R. & Dominguez, D. *Phys. Rev. Lett.* **76,** 2985–2988 (1996).
5. Olson, C. J., Reichhardt, C. & Nori, F. *Phys. Rev. B* **56,** 6175–6194 (1997).
6. Higgins, M. J. & Bhattacharya, S. *Physica C* **257,** 232–254 (1996).
7. Matsuda, T. *et. al. Science* **271,** 1393–1395 (1996).

Supplementary information is available on *Nature*'s World-Wide Web site (http://www.nature.com) or as paper copy from the London editorial office of *Nature*.

Role of the giant panda's 'pseudo-thumb'

The way in which the giant panda, *Ailuropoda melanoleuca*, uses the radial sesamoid bone — its 'pseudo-thumb' — for grasping makes it one of the most extraordinary manipulation systems in mammalian evolution[1–5]. The bone has been reported to function as an active manipulator, enabling the panda to grasp bamboo stems between the bone and the opposing palm[2,6–8]. We have used computed tomography, magnetic resonance imaging (MRI) and related techniques to analyse a panda hand. The three-dimensional images we obtained indicate that the radial sesamoid bone cannot move independently of its articulated bones, as has been suggested[1–3], but rather acts as part of a functional unit of manipulation. The radial sesamoid bone and the accessory carpal bone form a double pincer-like apparatus in the medial and lateral sides of the hand, respectively, enabling the panda to manipulate objects with great dexterity.

Schematic drawings based on computed-tomography and three-dimensional reconstructed images (Fig. 1a–c) explain the grasping mechanism used by the giant panda. Three-dimensional data obtained from artificial grasping of a carcass hand show that the radial sesamoid bone does not abduct or adduct independently of the first metacarpal and the radial carpal bones, and that the accessory carpal bone does not move substantially in the gripping action. When the movement is compared for open and gripping hands, the radial sesamoid bone, the first metacarpal and the radial carpal are actually moulded into a single bone, and the accessory carpal bone and the ulna constitute a single functional unit. When the hand is opened, the radial sesamoid bone and the accessory carpal bone therefore protrude at different angles from the plane of the palm (Fig. 1a).

The radial carpal bone forms an enlarged articulated surface to the distal end of the radius. In the gripping action, the five long phalanges are crooked (Fig. 1b) while the panda flexes the wrist joint (Fig. 1c). This wrist flexion means that the radial sesamoid bone is parallel to the accessory carpal bone, and the distal phalanges are parallel with the radius and ulna. This arrangement gives the panda a degree of opposability between the phalanges and the functional unit comprising the radial sesamoid bone and the accessory carpal bone (Fig. 1c).

The radial sesamoid bone and the accessory carpal bone do not move independently of their articulated bones in the grasping action, but constitute a functional unit with the first metacarpal and the radial carpal, and the ulna, respectively. The panda has three functional units: the RRM complex (radial sesamoid – radial carpal – first metacarpal), the AU complex (accessory carpal – ulna), and the phalanges (Fig. 1a–c). The RRM complex flexes and the radial sesamoid bone becomes parallel with the accessory carpal bone, and the phalanges bend and hold things in the hollow of the hand during the grasping action. The phalanges make a pincer-like apparatus with the RRM complex in the medial part of the hand, and another with the AU complex in the lateral part of the hand (Fig. 1a–c). It is this pair of 'pincers' that gives the panda its manual dexterity.

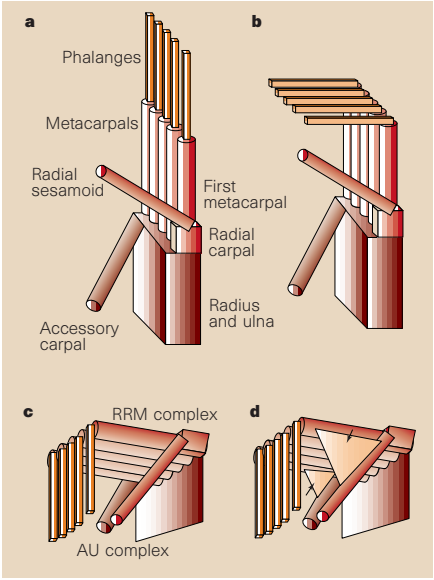

Figure 1 Schematic drawings of the grasping mechanism of the giant panda (medial view of right hand, with the proximal direction at the bottom). **a,** Hand open. **b,** Hand open but with the phalanges flexed. **c,** The grasping action (from a small palmar angle). The radial sesamoid and accessory carpal bones do not move independently of their articulated bones in the grasping action, but constitute two functional units: the RRM complex (see text) in the medial part of the hand, and the AU complex (see text) in the lateral part. Pincer-like structures are made by the phalanges and the RRM complex in the medial part, and by the phalanges and the AU complex in the lateral part. **d,** As **c**, but showing the muscles in the pincer-like structures on both sides of the grasped hand (arrows).

The MRI images indicate that the *abductor pollicis brevis* and the *opponens pollicis* muscles serve as a cushion for objects grasped between the radial sesamoid bone and the first metacarpal. The two muscle bundles surround the objects, increase friction between the hand and the objects, and alter the size and shape of the area in the hand. In the lateral part of the palm, the *abductor digiti quinti* muscle is well developed between the accessory carpal bone, the fifth metacarpal and the phalanges[2]. We suggest that the muscle pads may also help the panda to receive and hold objects grasped by the AU complex (Fig. 1d).

Our idea that the radial sesamoid bone does not function independently, but as part of the RRM functional complex, takes no account of the role of its abductor and adductor muscles. We suggest that the three functional units, and the double-pincer-like apparatus of which they are made, can be completely controlled only by the same muscular system that is found in other bear species. The wrist flexion and the manipulation of the double-pincer apparatus have

been observed in three live individuals in Ueno Zoological Park in Tokyo, Japan, when they were grasping food plants.

We have shown that the hand of the giant panda has a much more refined grasping mechanism than has been suggested in previous morphological models[2,6–9].

Hideki Endo*, Daishiro Yamagiwa†, Yoshihiro Hayashi†, Hiroshi Koie‡, Yoshiki Yamaya‡, Junpei Kimura‡

**Department of Zoology, National Science Museum, Tokyo, Shinjuku, Tokyo 169, Japan*
e-mail: endo@kahaku.go.jp
†Department of Veterinary Anatomy, University of Tokyo, Tokyo 113, Japan
‡College of Bioresource Sciences, Nihon University, Kanagawa 252, Japan

1. Lankester, E. R. & Lydekker, R. *Trans. Linn. Soc.* **8,** 163–171 (1901).
2. Davis, D. D. *Field. Zool. Mem.* **3,** 41–124, 146-198 (1964).
3. Gould, S. J. *Nat. Hist.* **87,** 20–30 (1978).
4. Pocock, R. I. *Nature* **143,** 206 (1939).
5. Endo, H. *et al. J. Anat.* **189,** 587–592 (1996).
6. Wood-Jones, F. *Nature* **143,** 157 (1939).
7. Wood-Jones, F. *Proc. Zool. Soc. Lond. B* **109,** 113–129 (1939).
8. Beijing Zoo *Morphology of the Giant Panda. Systematic Anatomy and Organ Histology* 148–152 (Science, Beijing, 1986).
9. Bourlière, F. *Traité de Zoologie XVII* 234–236 (Masson, Paris, 1955).

Yeast cell-type regulation of DNA repair

The mating-type locus (*MAT*) in the yeast *Saccharomyces cerevisiae* provides information about whether cells are of the **a** or α mating type, and genes at this locus encode transcriptional regulators that determine the phenotypes associated with the different cell types[1]. In **a**/α diploid cells, the **a**1/α2 repressor is formed, which inhibits haploid-specific gene expression and indirectly promotes meiosis. Mutations in *SIR* (silent information regulator) genes cause a loss of both heterochromatin and transcriptional silencing, resulting in the expression of cryptic **a** and α genes resident at the *HML* and *HMR* loci. As a result, *sir* mutant strains have the properties of **a**/α diploids.

Non-homologous end-joining (NHEJ) is required in mammals both for *V*(*D*)*J* recombination[2] and for repairing double-stranded DNA breaks. NHEJ also occurs in yeast[3,4], and it has been reported that Sir proteins are required for this process[5,6]. This observation was interpreted to mean that Sir proteins are involved directly in NHEJ, perhaps by forming a heterochromatin-like structure at double-stranded breaks. But we have found evidence for an alternative interpretation: that the **a**/α-state regulates NHEJ and that *sir* mutations affect NHEJ indirectly.

To distinguish between these two possibilities, we performed plasmid-rejoining assays. Plasmids that were linearized by restriction enzymes and contained a double-stranded break in vector sequences lacking homology to the yeast genome were transformed into yeast. The frequency of transformants was used as a measure of NHEJ[5,6]. Results obtained from SIR^+ and sir^- strains were consistent with previous findings[5,6]. NHEJ in sir^- strains was 20-fold less efficient than in wild-type strains (Table 1). However, assays performed in SIR^+ and sir^- strains in which all mating-type genes had been inactivated by a promoter deletion (*hml*αΔp *mat***a**Δp *hmr*αΔp, abbreviated here as $a^-a^-a^-$) revealed that the absence of mating-type heterozygosity suppressed the defect in NHEJ exhibited by the sir^- strains (Table 1).

We performed plasmid-rejoining assays on two SIR^+ diploid strains, an **a**/α diploid and a non-**a**/α diploid (*mat***a**Δp/*MAT*α, in which only α information is expressed). The non-**a**/α diploid strain accomplished NHEJ tenfold more efficiently than the **a**/α diploid (Table 1). NHEJ was therefore controlled by mating-type heterozygosity, and no cell-type-independent effect of *sir* mutations was detected.

Table 1 **Efficiency of non-homologous end-joining in haploid and diploid strains**

Strain	Genotype	Relative efficiency of NHEJ
Haploid strains		
JRY2334	wild type	100
JRY4563	*sir2::TRP1*	7 ± 1
JRY3289	*sir3::TRP1*	4 ± 1
JRY4580	*sir4::TRP1*	6 ± 3
JRY3658	*hml***a**Δp *mat***a**Δp *hmr***a**Δp	66 ± 22
JRY6348	*hml***a**Δp *mat***a**Δp *hmr***a**Δp *sir2::TRP1*	114 ± 2
JRY3606	*hml***a**Δp *mat***a**Δp *hmr***a**Δp *sir3::TRP1*	64 ± 7
JRY6349	*hml***a**Δp *mat***a**Δp *HMR***a** *sir4::TRP1*	130 ± 4
Diploid strains		
JRY5384	*MAT***a**/*MAT*α	10 ± 2
JRY6328	*mat***a**Δp/*MAT*α	100

All strains were isogenic to W303-1a (*MAT***a** *ade2-1 can1-100 his3-11,15 leu2-3,112 trp1-1 ura3-1 rad5-535*) unless indicated. Strains were transformed using *Hin*dIII-digested pRS316 or pRS416 by the lithium acetate method and plated onto supplemented minimal plates selecting for uracil prototrophy. Efficiency of non-homologous end-joining (NHEJ) was calculated by normalizing the number of transformants obtained to the number of transformants obtained in parallel transformations with supercoiled plasmid. The average absolute efficiency of NHEJ in strains JRY2334 and JRY6328 were 89% and 22%, respectively. Data are mean ± standard deviation of two or three independent experiments.

The defect in NHEJ found in **a**/α cells indicates that a gene required for NHEJ was regulated by the **a**1/α2 repressor. RNA blot analysis of *HDF1*, *HDF2*, *DNL4*, *XRS2* and *MRE11*, the leading candidate genes[7–10] in wild-type, *sir3*, $a^-a^-a^-$ and $a^-a^-a^-$ *sir3* strains, revealed that all five genes were comparably expressed in *SIR3* and *sir3* strains (data not shown). These genes are therefore not relevant targets for the **a**1/α2 repression of NHEJ.

Our results provide evidence against a direct role for heterochromatin formation in NHEJ, indicating instead that the efficiency of NHEJ is controlled by cell type. But our data do not exclude the possibility that different strains might yield different results: indeed, the W303 strain we used contains a mild *rad5* mutation. However, the **a**/α regulation of NHEJ found here can explain problems associated with DNA repair in yeast. Diploid cells that suffer a double-stranded break have a homologous partner that can perform a homology-driven recombinational repair process. In cells that have more than one double-stranded break, NHEJ could lead to exchange-type aberrations[11], indicating that homology-driven repair should be the preferred pathway. But haploid cells in the G1 phase of the cell cycle lack homologues and so rely on NHEJ. With NHEJ under the control of the **a**1/α2 repressor, a yeast cell could adapt the repair process, using the NHEJ pathway primarily when homology-driven repair is not possible. This would require an **a**1/α2-repressed gene that is important for NHEJ. Alternatively, **a**1/α2 could inhibit NHEJ indirectly by upregulating the *RAD52* homologous repair pathway to outcompete the NHEJ pathway for the repair of double-stranded breaks.

Stefan U. Åström*, Sara M. Okamura, Jasper Rine

Department of Molecular and Cell Biology, University of California, Berkeley, Berkeley, California 94720, USA
e-mail: jrine@uclink4.berkeley.edu
**Present address: Umeå Center for Molecular Pathogenesis, Umeå University, S-901 87 Umeå, Sweden*

1. Herskowitz, I., Rine, J. & Strathern, J. *The Molecular Biology of the Yeast* Saccharomyces (eds Jones, E. W., Pringle, J. R. & Broach, J. R.) 583–656 (Cold Spring Harbor Laboratory Press, NY, 1992).
2. Lieber, M. R. *Curr. Biol.* **6,** 134–136 (1996).
3. Milne, G. T., Jin, S., Shannon, K. B. & Weaver, D. T. *Mol. Cell. Biol.* **16,** 4189–4198 (1996).
4. Boulton, S. J. & Jackson, S. P. *EMBO J.* **15,** 5093–5103 (1996).
5. Tsukamoto, Y., Kato, J. & Ikeda, H. *Nature* **388,** 900–903 (1997).
6. Boulton, S. J. & Jackson, S. P. *EMBO J.* **17,** 1819–1828 (1998).
7. Feldmann, H. & Winnacker, E. L. *J. Biol. Chem.* **268,** 12895–12900 (1993).
8. Feldmann, H. *et al. J. Biol. Chem.* **271,** 27765–27769 (1996).
9. Schiestl, R. H., Zhu, J. & Petes, T. D. *Mol. Cell. Biol.* **14,** 4493–4500 (1994).
10. Wilson, T. E., Grawunder, U. & Lieber, M. R. *Nature* **388,** 495–498 (1997).
11. Friedl, A. A., Kiechle, M., Fellerhoff, B. & Eckardt-Schupp, F. *Genetics* **148,** 975–988 (1998).